

# Ferro- to antiferromagnetic crossover angle in diphenoxido and carboxylato bridged trinuclear $\text{Ni}^{\text{II}}$ - $\text{Mn}^{\text{II}}$ complexes: Experimental observations and theoretical rationalization

Piya Seth,<sup>a</sup> Albert Figuerola,<sup>\*b,c</sup> Jesús Jover,<sup>b,d</sup> Eliseo Ruiz,<sup>b,d</sup> and Ashutosh Ghosh<sup>\*a</sup>

<sup>a</sup> *Department of Chemistry, University College of Science, University of Calcutta, 92, A.P.C. Road, Kolkata-700 009, India; e-mail: ghosh\_59@yahoo.com*

<sup>b</sup> *Departament de Química Inorgànica, Universitat de Barcelona, Martí i Franquès 1-11, 08028 Barcelona, Spain; e-mail: albert.figuerola@qi.ub.edu*

<sup>c</sup> *Institut de Nanociència i Nanotecnologia (IN2UB), Universitat de Barcelona, Martí i Franquès 1-11, 08028 Barcelona, Spain*

<sup>d</sup> *Institut de Recerca de Química Teòrica i Computacional, Universitat de Barcelona, Diagonal 645, E-08028 Barcelona, Spain*

---

## Abstract

Three new trinuclear heterometallic  $\text{Ni}^{\text{II}}$ - $\text{Mn}^{\text{II}}$  complexes have been synthesized using  $[\text{NiL}]$  metalloligand where  $\text{H}_2\text{L} = \text{N,N'}$ -bis(salicylidene)-1,3-propanediamine. The complexes  $[(\text{NiL})_4\text{Mn}_2(\text{OCn})_4(\text{CH}_3\text{OH})_4] \cdot 2\text{CH}_3\text{OH}$  (**1**),  $[(\text{NiL})_4\text{Mn}_2(\text{OPh})_4(\text{CH}_3\text{OH})_2] \cdot \text{H}_2\text{O}$  (**2**) and  $[(\text{NiL})_4\text{Mn}(\text{OSal})_2(\text{CH}_3\text{OH})_2]$  (**3**) (where  $\text{OCn} = \text{cinnamate}$ ,  $\text{OPh} = \text{phenylacetate}$ ,  $\text{OSal} = \text{salicylate}$ ) have been structurally characterized. In all three complexes, in addition to the double phenoxido bridge, the two terminal  $\text{Ni}^{\text{II}}$  atoms are linked to the central  $\text{Mn}^{\text{II}}$  by means of *syn-syn* bridging carboxylate, giving rise to a linear structure. Complexes **1** and **2** with Ni-O-Mn angle of 97.24 and 96.43° respectively exhibit ferromagnetic interactions ( $J_{\text{Ni-Mn}} = +1.38$  and  $+0.50 \text{ cm}^{-1}$  respectively) whereas **3** is antiferromagnetic ( $J_{\text{Ni-Mn}} = -0.24 \text{ cm}^{-1}$ ) having Ni-O-Mn angle of 98.51°. DFT calculations indicate that there is a clear magneto-structural correlation between Ni-O-Mn angle and  $J_{\text{Ni-Mn}}$  values which is in agreement with the experimental results.

---

## Introduction

Rational design and synthesis of oxido or phenoxido bridged molecular assemblies formed by a finite number of exchange-coupled paramagnetic centers have attracted the attention of inorganic chemists for long time. Majority of the species that have been studied are homometallic. Among them homonuclear  $\text{Cu}^{\text{II}}$ ,<sup>1</sup>  $\text{Ni}^{\text{II}}$ ,<sup>2</sup> and  $\text{Mn}^{\text{III}}$ <sup>3</sup> complexes derived from di-Schiff base ligands and various bridging coligands are of considerable interest because of their fascinating structural features and intriguing magnetic properties. These compounds also play a key role in deriving the magneto-structural correlations for oxido and/or phenoxido bridged metal complexes. From the experimental and theoretical results, it can be said that the magnetic exchange interactions in this class of compounds depend on several factors *e.g.* M-O-M angle, M-O distance, the effect of the asymmetry on the metal-bridge bonds, and the hinge distortion of the  $\text{M}_2\text{O}_2$  core.<sup>4</sup> DFT calculations showing the dependence of the coupling constant  $J$  on the phenoxido bridging angle in homometallic dinuclear  $\text{Cu}^{\text{II}}$ ,  $\text{Ni}^{\text{II}}$ ,  $\text{Mn}^{\text{III}}$  complexes are performed in details to quantify the respective contributions for ferro-/antiferromagnetic interactions. Both from theoretical calculations and experimental results, it has been found that for dinuclear  $\text{Cu}^{\text{II}}$  complexes ferromagnetism appears for a bridging Cu–O–Cu angle lower than  $92.4^\circ$ .<sup>1a</sup> The critical phenoxido bridging angle is  $93.5^\circ$  for  $\mu_2\text{-O}$  bridged dinuclear  $\text{Ni}^{\text{II}}$  complexes<sup>2a</sup> and  $101^\circ$  for  $\text{Mn}^{\text{III}}$  complexes.<sup>3d,e</sup>

The number of oxido/phenoxido bridged heterometallic  $\text{Cu}^{\text{II}}$ ,  $\text{Ni}^{\text{II}}$ , and  $\text{Mn}^{\text{III}}$  complexes of salen type Schiff base ligands are relatively less than the corresponding homometallic complexes. Moreover, in most of these complexes the metal ions are  $\text{Cu}^{\text{II}}\text{-Ni}^{\text{II}}$ <sup>5</sup> and  $\text{Cu}^{\text{II}}\text{-Mn}^{\text{II}}$ .<sup>6</sup> The number of  $\text{Ni}^{\text{II}}\text{-Mn}^{\text{II}}$  complexes with this type of ligands is relatively scanty and only very few of them are magnetically characterized. A recently updated CSD search reveals that the number of di-phenoxido bridged  $\text{Ni}^{\text{II}}\text{-Mn}^{\text{II}}$  complexes of salen type Schiff base ligand is eleven,<sup>7-9</sup> among which only two are magnetically characterized.<sup>7,8</sup> Between these two complexes, one having Ni–O–Mn angle of  $86.38^\circ$  is ferromagnetically coupled ( $J_{\text{Ni-Mn}} = +9.3 \text{ cm}^{-1}$ ) while the other one shows antiferromagnetic interactions ( $J_{\text{Ni-Mn}} = -0.30 \text{ cm}^{-1}$ ) with Ni–O–Mn angle of  $102.31^\circ$ . The results clearly suggest that a critical angle should be there in between and therefore it is worthy to design and synthesize some  $\text{Ni}^{\text{II}}\text{-Mn}^{\text{II}}$  heterometallic complexes with the phenoxido bridging

angle within the range 86-102°, so that one can have an idea of the critical angle for this system. An efficient strategy for synthesizing heterometallic complexes of salen type Schiff base ligand is to employ ‘metalloligand’ approach. The use of various bridging and/or terminally coordinating anionic coligands plays an important role in controlling the phenoxido bridging angle and consequently the magnetic coupling.<sup>10</sup> Recently, we reported some trinuclear Cu<sup>II</sup>–Mn<sup>II</sup> complexes using [CuL] ‘metalloligand’ (where H<sub>2</sub>L= N,N'- bis(salicylidene)-1,3-propanediamine). Although the Cu-O-Mn bridging angles in these complexes have been varied in a wide range of 92° to 101° by suitably selecting the anionic coligands, the antiferro- to ferromagnetic crossover angle was not detected.<sup>6e</sup> However, for Ni<sup>II</sup>-Mn<sup>II</sup> complexes the experimental search for critical angle should end in a success by narrowing down the range as both ferro and antiferromagnetically coupled complexes are known.<sup>7,8</sup> The aim of the present investigation is therefore, to synthesize some Ni<sup>II</sup>-Mn<sup>II</sup> complexes with the variation of phenoxido bridging angles and to study their magnetic properties. We would also like to substantiate the experimental magnetic coupling with the help of DFT studies which have rarely been done for such heterometallic compounds.

Herein we report the synthesis, crystal structure and magnetic properties of three new complexes [(NiL)<sub>4</sub>Mn<sub>2</sub>(OCn)<sub>4</sub>(CH<sub>3</sub>OH)<sub>4</sub>].2CH<sub>3</sub>OH (**1**), [(NiL)<sub>4</sub>Mn<sub>2</sub>(OPh)<sub>4</sub>(CH<sub>3</sub>OH)<sub>2</sub>].H<sub>2</sub>O (**2**) and [(NiL)<sub>4</sub>Mn(OSal)<sub>2</sub>(CH<sub>3</sub>OH)<sub>2</sub>] (**3**) where OCn = cinnamate, OPh = phenylacetate, OSal = salicylate. Among these complexes **1** and **2** have average Ni-O-Mn angle 97.24 and 96.43° respectively exhibiting ferromagnetic interactions with  $J_{Ni-Mn}$  values +1.38 and +0.50 cm<sup>-1</sup>. For **3** the Ni-O-Mn angle is 98.51° corresponding to antiferromagnetic interactions ( $J_{Ni-Mn}$  = -0.24 cm<sup>-1</sup>). For the title heterometallic complexes theoretical calculations support the experimentally observed fact that the Ni<sup>II</sup>–Mn<sup>II</sup> systems have a large tendency to show ferromagnetic coupling because of predominating orthogonally oriented magnetic orbitals of the two metal ions, and larger Ni-O-Mn angles (above 98°) are responsible for antiferromagnetic spin exchange.

## Experimental

**Synthesis of manganese carboxylates:** The three metal carboxylate salts viz. Mn(OCn)<sub>2</sub> Mn(OPh)<sub>2</sub>.H<sub>2</sub>O, and Mn(OSal)<sub>2</sub> were prepared by following the similar procedures. To an aqueous solution (30 mL) of corresponding carboxylic acids (148.16 mg of cinnamic acid,

136.15 mg of phenylacetic acid or 138.12 mg of salicylic acid) manganese carbonate (60.0 mg) was added in small portions with constant stirring with a glass rod until effervescence ceased. Then the mixture was warmed on a water bath for 10-15 min and filtered. The clear filtrate was kept over a water bath until a solid started to separate. The solution was then cooled to room temperature, and the crystalline solid product was filtered through suction and dried in vacuum. All other chemicals are commercial and were of reagent grade and used as received, without further purification.

**Synthesis of the Schiff-Base Ligand N,N'-Bis(salicylidene)-1,3-propanediamine (H<sub>2</sub>L):** The di-Schiff base ligand, H<sub>2</sub>L, was synthesized in our laboratory by standard methods.<sup>11</sup> Salicylaldehyde (1.05 mL, 10 mm) was mixed with 1,3-propanediamine (0.42 mL, 5 mm) in methanol (20 mL). The resulting mixture was refluxed for *ca.* 1.5 h and allowed to cool. The desired yellow crystalline ligand was filtered off, washed with methanol, and dried in a vacuum desiccator containing anhydrous CaCl<sub>2</sub>.

**Preparation of the 'metalloligand' [NiL]:** A mixture of H<sub>2</sub>L (1.432 g, 5 mM) in methanol and ammonia solution (10 mL, 20%) was added to a methanolic solution (20 mL) of Ni(ClO<sub>4</sub>)<sub>2</sub>·6H<sub>2</sub>O (1.825 g, 5 mM) to prepare the "ligand complex" [NiL] as previously reported.<sup>12</sup>

**Synthesis of complexes 1-3:** To a 20 mL methanolic solution of [NiL] (0.321 g, 1 mM) an aqueous solution (5 mL) of Mn(OCn)<sub>2</sub> (0.175 g, 0.5 mM), Mn(OPh)<sub>2</sub>·H<sub>2</sub>O (0.172 g, 0.5 mM) and Mn(OSal)<sub>2</sub> (0.165 g, 0.5 mM) for **1**, **2** and **3** respectively were added and stirred for *ca.* 1 h at room temperature. A green precipitate separated from the reaction mixture in each case was filtered and the respective filtrates were allowed to stand overnight. Deep green colored X-ray quality single-crystals appeared at the wall of the vessel on slow evaporation of the solvent in each case. The crystals were isolated, washed with methanol, and dried in a desiccator containing anhydrous CaCl<sub>2</sub>.

**Complex 1:** Yield: 0.410g (71%) C<sub>56</sub>H<sub>61</sub>N<sub>4</sub>O<sub>12</sub>Ni<sub>2</sub>Mn (1154.41): calcd C, 58.26; H, 5.33; N, 4.85; found C, 58.12; H, 5.29; N, 4.73. IR (KBr pellet, cm<sup>-1</sup>) 1638  $\nu$ (C=N), 1578  $\nu_{as}$ (COO), 1468  $\nu_s$ (COO).  $\lambda_{max}$  (MeOH, nm) 350, 409 and 599.

**Complex 2:** Yield: 0.388 g (74%) C<sub>51</sub>H<sub>50</sub>N<sub>4</sub>O<sub>10</sub>Ni<sub>2</sub>Mn (1051.26): calcd C, 58.27; H, 4.79; N, 5.33; found C, 58.18; H, 4.70; N, 5.26. IR (KBr pellet, cm<sup>-1</sup>) 1635  $\nu$ (C=N), 1588  $\nu_{as}$ (COO), 1469  $\nu_s$ (COO).  $\lambda_{max}$  (MeOH, nm) 356, 407 and 592.

**Complex 3:** Yield: 0.297 g (68%) C<sub>84</sub>H<sub>82</sub>N<sub>8</sub>O<sub>16</sub>Ni<sub>4</sub>Mn (1749.28): calcd C, 57.67; H, 4.72; N, 6.41; found C, 57.56; H, 4.65; N, 6.35. IR (KBr pellet, cm<sup>-1</sup>) 1625  $\nu$ (C=N), 1541  $\nu_{as}$ (COO), 1463  $\nu_s$ (COO).  $\lambda_{max}$  (MeOH, nm) 349, 408, 597.

**Physical measurements:** Elemental analyses (C, H, and N) were performed using a Perkin-Elmer 240C elemental analyzer. IR spectra in KBr (4000–500 cm<sup>-1</sup>) were recorded using a Perkin-Elmer RXI FTIR spectrophotometer. Temperature-dependent molar susceptibility measurements of powdered samples of **1-3** were carried out at the “Servei de Magnetoquímica (Universitat de Barcelona)” in a Quantum Design SQUID MPMSXL susceptometer with an applied field of 3000 and 198 G in the temperature ranges 2–300 and 2–30 K, respectively.

**Computational details:** To calculate the exchange interactions, a phenomenological Heisenberg-Dirac-van Vleck Hamiltonian was used, excluding the terms relating to magnetic anisotropy, to describe the exchange coupling in a general polynuclear complex:

$$\hat{H} = - \sum_{a < b} J_{ab} \hat{S}_a \hat{S}_b \quad (1)$$

where  $\hat{S}_a$  and  $\hat{S}_b$  are the spin operators of the different paramagnetic cations. The  $J_{ab}$  parameters are the pairwise coupling constants between the paramagnetic centres of the molecule. Basically, we need to calculate the energy of  $n+1$  spin distributions for a system with  $n$  different exchange coupling constants.<sup>13-17</sup> These energy values allow us to build up a system of  $n$  equations in which the  $J$  values are the unknowns. In the present study, three calculations were performed in order to obtain the two exchange coupling constants of the MnNi<sub>2</sub> complexes. They correspond to the high-spin  $S = 9/2$  state, one  $S = 1/2$  wave function flipping the spin of the central manganese atom, and finally one  $S = 5/2$  with the spin inversion of the two external nickel atoms. Theoretical Calculations were performed with the hybrid B3LYP functional<sup>18</sup> as implemented in Gaussian09 code<sup>19</sup> using a guess function generated with the Jaguar 7.0 code,<sup>20</sup> which employs a procedure that allows us to determine individually the local charges and

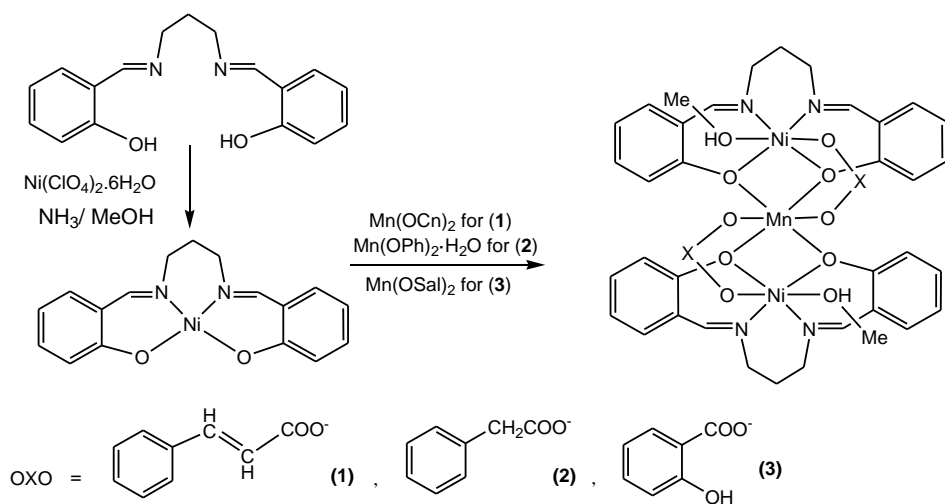
multiplicities of the atoms, including the ligand field effects.<sup>21</sup> A triple- $\zeta$  all-electron Gaussian basis set was used for all the atoms.<sup>22</sup>

**Crystal data collection and refinement:** Suitable single crystals of complexes **1-3** were mounted on a Bruker-AXS SMART APEX II diffractometer equipped with a graphite monochromator and Mo-K $\alpha$  ( $\lambda = 0.71073$  Å) radiation. The crystals were positioned at 60 mm from the CCD. 360 Frames were measured with a counting time of 10 s. The structures were solved by the Patterson method using the SHELXS 97. Subsequent difference Fourier synthesis and least-square refinement revealed the positions of the remaining non-hydrogen atoms that were refined with independent anisotropic displacement parameters. Hydrogen atoms were placed in idealized positions and their displacement parameters were fixed to be 1.2 times larger than those of the attached non-hydrogen atom. Absorption corrections were carried out using the SADABS program.<sup>23</sup> All calculations were carried out using the SHELXS 97,<sup>24</sup> SHELXL 97,<sup>25</sup> PLATON 99,<sup>26</sup> ORTEP-32<sup>27</sup> and WinGX system Ver-1.64.<sup>28</sup> Data collection, structure refinement parameters and crystallographic data for the three complexes are given in Table 1.

## Results and Discussions

**Syntheses, IR and Electronic spectra of the complexes:** Three new Ni<sup>II</sup>–Mn<sup>II</sup> carboxylate complexes derived from Schiff base H<sub>2</sub>L, were synthesized by following similar procedure. For this purpose, we have first prepared the ‘metalloligand’ [NiL] by a reported procedure.<sup>12</sup> An aqueous solution of respective manganese carboxylates were prepared by warming them in 5ml of water and were mixed with a 20 mL of methanolic solution of [NiL]. The solutions were stirred for about an hour and then filtered. From the clear filtrate, X-ray quality single crystals were obtained after 2-3 days. Besides elemental analysis, all three complexes were characterized by IR spectroscopy. For **1**, **2**, and **3** a strong and sharp band appeared at 1638, 1635 and 1625 cm<sup>-1</sup>, respectively, due to azomethine  $\nu(\text{C}=\text{N})$ . Other peaks due to asymmetric and symmetric stretching of carboxylate are observed at 1578, 1468 cm<sup>-1</sup> (in **1**) 1588, 1469 cm<sup>-1</sup> (in **2**) 1541, 1463 cm<sup>-1</sup> (in **3**) respectively. Electronic spectra of the three complexes in methanol solvent are similar having two strong peaks at 350, 409 nm (in **1**), 356, 407 nm (in **2**), 349, 408 nm (in **3**) which correspond to ligand to metal charge transfer transitions. Another strong absorption band

is observed at 599, 592 and 597 nm for **1**, **2** and **3** respectively which can be assigned to the d–d transitions in Ni<sup>II</sup> complexes.



**Scheme 1** Formation of complexes **1–3**.

**Description of structures:** The X-ray crystal structure of **1** reveals that it consists of two similar centrosymmetric trinuclear units **1A** and **1B** having the same composition  $[(\text{NiL})_2\text{Mn}(\text{OCn})_2(\text{CH}_3\text{OH})_2] \cdot \text{CH}_3\text{OH}$ . Here, both the units contain a six-coordinate Mn<sup>II</sup> in a distorted octahedral environment together with two six-coordinated octahedral Ni<sup>II</sup> with equivalent geometries. The manganese atom is situated at the centre of inversion and is bonded to four oxygen atoms from the two ligands L, at distances ranging 2.158(2)–2.170(2) Å in **1A** and 2.120(2)–2.212(2) Å in **1B**, that form the basal plane of the Mn(II) while the trans axial positions are occupied by the oxygen atom O(4) (in **1A**) and O(8) (in **1B**) of the *syn-syn* bridging cinnamate at distances of 2.210(2) and 2.225(2) in **1A** and **1B** respectively. (Table 2)

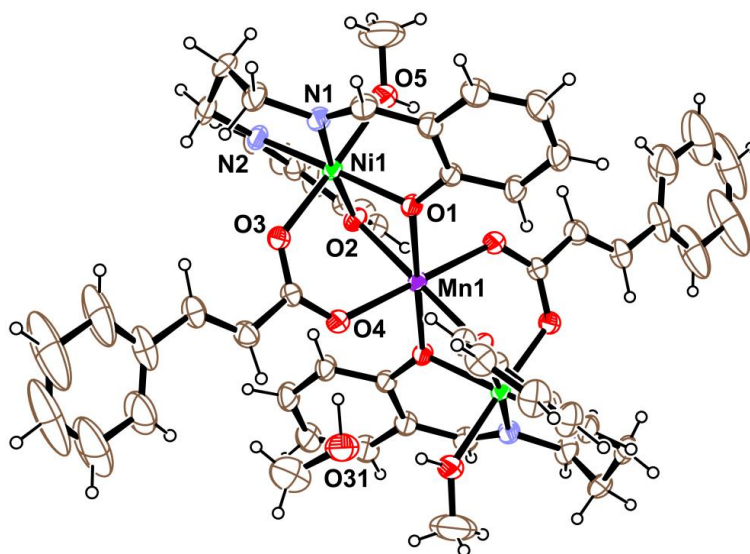


**Figure 1.** ORTEP-3 view of the centrosymmetric trinuclear structure of **1A** with ellipsoids at 30% probability. There are two trimers with equivalent structures, only one is shown.

The two terminal nickel atoms are bonded to four donor atoms (O(1), O(2), N(1), N(2) in **1A** and (O(6), O(7), N(3), N(4) in **1B**) of the ligand L, making up the equatorial plane with Ni–O distances in the range of 2.023(2)–2.028(2) Å in **1A**, 2.017(2)–2.020(2) Å in **1B** and Ni–N distances of 2.024(2)–2.035(2) Å in **1A**, 2.022(2)–2.030(2) Å in **1B**. One of the axial positions is occupied by oxygen atom (O(3) in **1A**, O(9) in **1B**) of the *syn-syn* bridging cinnamate at distances of 2.055(2), and 2.052(2) Å respectively. The other axial positions of the nickel atoms are bonded to the oxygen atom of the solvent methanol at distances of 2.153(2) in **1A** and 2.147(3) Å in **1B**. The mean deviation of four donor atoms in the basal plane from their respective mean plane are 0.003Å (in **1A**), 0.031Å (in **1B**) while the Ni atom is deviated by 0.024(1) Å to the direction of the axial O(3) in **1A** and 0.004(1) Å towards O(9) in **1B**. Ni...Mn distance is 3.149(4) Å in **1A** and 3.133(4) Å in **1B**. Two Ni–O–Mn bridging angles are 97.29(7), 97.74(7)° in **1A** and 95.52(7), 98.36(8)° in **1B**.

Complex **2** also consists of two centrosymmetric trinuclear units [(NiL)<sub>2</sub>Mn(OPh)<sub>2</sub>(CH<sub>3</sub>OH)<sub>2</sub>].H<sub>2</sub>O (**2A**) and [(NiL)<sub>2</sub>Mn(OPh)<sub>2</sub>] (**2B**), but the compositions of the units are different. Each of the two units contains two terminal Ni<sup>II</sup> atoms and a central Mn<sup>II</sup> in a linear disposition. Both of them contain a six-coordinated manganese in a distorted octahedral environment at the centre of inversion and is bonded to four oxygens from the two ligands L, at



distances ranging 2.158(2)-2.175(2) Å in **2A** and 2.161(2)-2.163(2) Å in **2B**, that form the basal plane of the Mn(II). The trans axial positions are occupied by the oxygen atom O(4) (in **2A**) and O(8) (in **2B**) of the *syn-syn* bridging phenylacetate at distances of 2.199(2) and 2.138(2) Å in **2A** and **2B** respectively. (Table 2)

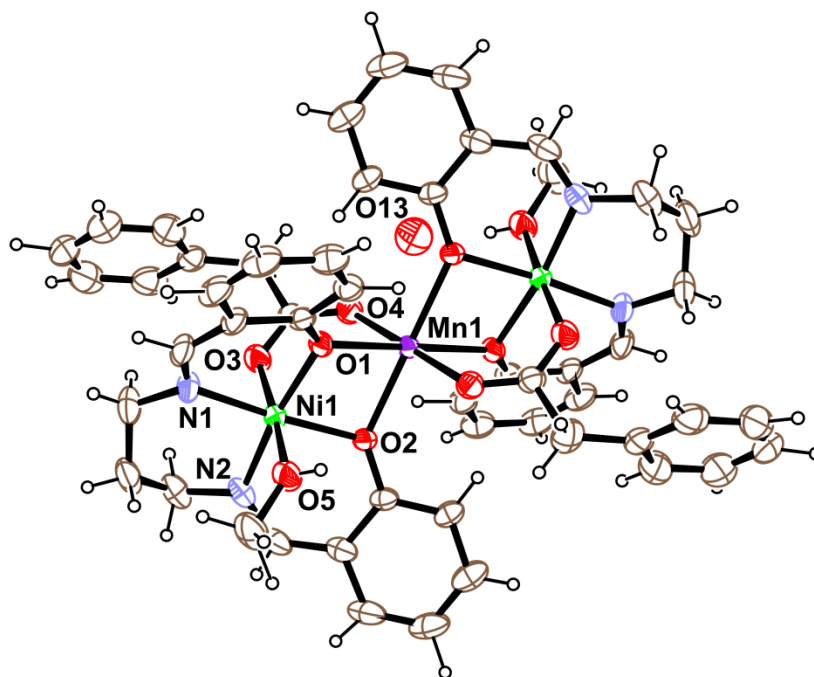


**Figure 2.** ORTEP-3 view of the centrosymmetric trinuclear structure of **2A** with ellipsoids at 30% probability. There are two trimers with equivalent structures, only one is shown.

The two terminal nickel atoms are bonded to four donor atoms (O(1), O(2), N(1), N(2) in **2A** and (O(6), O(7), N(3), N(4) in **2B**) of the tetradentate ligand L, making up the equatorial plane with Ni–O distances in the range of 2.016(2)-2.022(2) Å in **2A**, 1.999(2)-2.002(2) Å in **2B** and Ni–N distances of 2.016(3)-2.021(3) Å in **2A** and 2.014(2)- 2.017(2) Å in **2B**. The fifth coordination site is occupied by bridging oxygen atom (O(3) in **2A**, O(9) in **2B**) of the *syn-syn* bridging phenylacetate at distances of 2.054(3) and 1.995(2) Å in **2A** and **2B** respectively. The other axial position of the nickel atoms in **2A** is bonded to the oxygen atom of the solvent methanol with Ni(1)-O(5) distance 2.153(3) Å whereas this second axial position is vacant in **2B**. Thus the Ni atoms are hexa-coordinated with a distorted octahedral environment in **2A**, whereas penta-coordinated in **2B** with a geometry closer to the square pyramid as indicated by the

Addison parameter ( $\tau = 0.067$ ). The  $\tau$  is 0 for an ideal square pyramid and 1 for a trigonal bipyramid.<sup>29</sup> The mean deviations of four donor atoms in the basal plane from their respective mean plane are 0.005, 0.042 Å in **2A** and **2B** respectively. The Ni atom is deviated by 0.040(1) Å to the direction of the axial O(3) in **2A** and -0.271(1) Å to the direction of the axial O(9) in **2B**. Ni...Mn distance is 3.135(6) Å in **2A** and 3.091(5) Å in **2B**. Two Ni-O-Mn bridging angles are 96.58(8), 97.34(8)° in **2A** and 95.83(8), 95.87(7)° in **2B**.

The X-ray crystal structure analysis shows that **3** contains two units namely  $[(\text{NiL})_2\text{Mn}(\text{OSal})_2(\text{CH}_3\text{OH})_2]$  (**3A**) and  $[\text{NiL}]$  (**3B**). Of them, **3A** consists of trinuclear centrosymmetric structure containing two terminal  $\text{Ni}^{\text{II}}$  atoms and a central  $\text{Mn}^{\text{II}}$  in a linear disposition. The octahedral manganese atom is bonded to four oxygen atoms from the two ligands L, at distances ranging 2.171(2)-2.174(2) Å, that form the basal plane of the  $\text{Mn}^{\text{II}}$  while the trans axial positions are occupied by the oxygen atom O(4) of the *syn-syn* bridging salicylate at distances of 2.185(2) Å. The two terminal nickel atoms are bonded to four donor atoms (O(1), O(2), N(1), and N(2)) of the ligand L, making up the equatorial plane with Ni(1)-O distance in the range of 2.006(2)-2.016(2) Å and Ni-N distance 2.037(2)-2.042(2) Å. One of the axial positions is occupied by bridging oxygen atom O(3) of *syn-syn* salicylate at 2.095(2) Å. The other axial position of the nickel atoms are also bonded to the oxygen atom of the solvent methanol with Ni(1)-O(5) distance 2.185(2) Å that completes a distorted octahedral environment around Ni atom. The mean deviation of four donor atoms in the basal plane from their respective mean plane are 0.030 Å while the Ni atom is deviated by 0.008(1) Å to the direction of the axial O(3). Ni...Mn distance is 3.171(1) Å and two Ni-O-Mn bridging angles are 98.31(7) and 98.70(7)°. (Table 2)

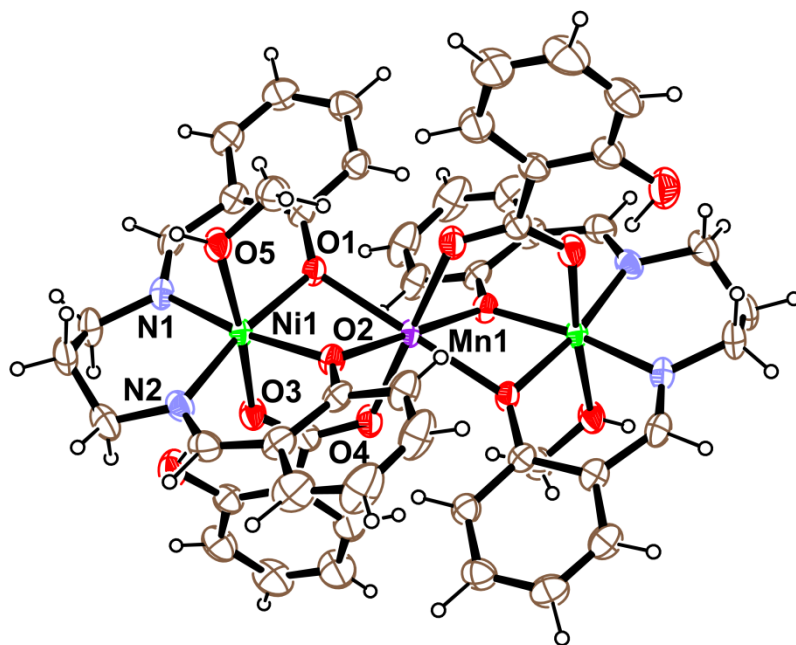


**Figure 3.** ORTEP-3 view of the centrosymmetric trinuclear structure of **3A** with ellipsoids at 30% probability.

**3B** consists of a mononuclear [NiL] unit where four-coordinated square planar nickel is bonded to the donor atoms O(6), O(7), N(3), N(4) of L with Ni(2)–O distances in the range 1.845(3)–1.862(2) Å and Ni(2)–N distances in the range 1.889(3)–1.900(5) Å. These distances are comparatively shorter than the corresponding distances in **1A**, **1B**, **2A**, **2B** and **3A** which is quite usual for square planar geometry.<sup>30</sup> The  $\tau_4$  value for Ni(2) is 0.154 which indicates slightly distorted square planar geometry around it.<sup>31</sup>

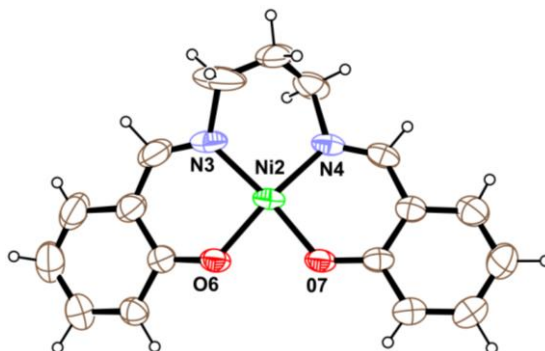


**Figure 4.** ORTEP-3 view of the centrosymmetric trinuclear structure of **3B** with ellipsoids at 30% probability.

**Magnetic Properties.** Magnetic measurements in complexes **1** and **2** show clear ferromagnetic interactions between Ni<sup>II</sup> and Mn<sup>II</sup> ions within the complexes, while antiferromagnetic exchange becomes obvious in complex **3**. Temperature-dependent molar susceptibility measurements on polycrystalline samples of **1-3** were carried out in an applied field of 0.3 T in the temperature range 1.9-300 K. The data are shown in the  $\chi_M T$  versus  $T$  plot in Figure 5, where  $\chi_M$  is the molar magnetic susceptibility and  $T$  is the absolute temperature. The room temperature values of  $\chi_M T$  for compounds **1-3** are 6.67, 6.61 and 6.63 cm<sup>3</sup>mol<sup>-1</sup>K respectively, slightly higher than the 6.4 cm<sup>3</sup>mol<sup>-1</sup>K value expected for non-interacting Ni<sup>II</sup>-Mn<sup>II</sup>-Ni<sup>II</sup> trinuclear units. For complexes **1** and **2**, the  $\chi_M T$  values increase with decreasing temperature until they reach a maximum of 9.47 cm<sup>3</sup>mol<sup>-1</sup>K at 4.5 K for **1** and 7.43 cm<sup>3</sup>mol<sup>-1</sup>K at 6 K for **2**. Below these temperatures, the value of  $\chi_M T$  drops sharply. On the other hand, the  $\chi_M T$  values measured for complex **3** are kept approximately constant down to 50 K, temperature below that they suddenly drop. In order to quantitatively interpret these data, simulations of the experimental curves were done by using the MAGPACK program as shown in Figure 5.<sup>32</sup> A Hamiltonian of the type  $H = -J[S_I S_2 + S_I S_3]$ , where  $S_I = S_{Mn}$  and  $S_2 = S_3 = S_{Ni}$ , was used for the simulations. In the model, the crystallographic equivalence of the two Ni<sup>II</sup> ions in the trinuclear unit was considered by assigning one single  $g$  value for that ion. Additionally, one single set of magnetic parameters was deduced for each of the studied compounds, regardless of the presence of two non-equivalent Ni<sub>2</sub>Mn trinuclear molecules in the unit cell in **1** and **2**. Simulations were carried out including a zero field splitting ( $D$ ) value for the two Ni<sup>II</sup> ions and considering that the exchange coupling between these two terminal ions was zero ( $J_{Ni-Ni} = 0$  cm<sup>-1</sup>). Moreover, a term accounting for intermolecular interactions ( $zJ'$ ) was also included. The best agreement between experimental and simulated curves was obtained with the following sets of parameters:  $g_{Ni} = 2.10$ ,  $g_{Mn} = 2.00$ ,  $D_{Ni} = 4.0$  cm<sup>-1</sup>,  $J_{Ni-Mn} = 1.38$  cm<sup>-1</sup> and  $zJ' = -0.06$  cm<sup>-1</sup> for complex **1**;  $g_{Ni} = 2.10$ ,  $g_{Mn} = 2.00$ ,  $D_{Ni} = 4.0$  cm<sup>-1</sup>,  $J_{Ni-Mn} = 0.50$  cm<sup>-1</sup> and  $zJ' = -0.06$  cm<sup>-1</sup> for complex **2**; and  $g_{Ni} = 2.10$ ,  $g_{Mn} = 2.00$ ,  $D_{Ni} = 4.0$  cm<sup>-1</sup>,  $J_{Ni-Mn} = -0.24$  cm<sup>-1</sup> and  $zJ' = -0.03$  cm<sup>-1</sup> for complex **3**. The  $D$  parameter was fixed in the simulations and assumed to have the same value for complexes **1-3** in order to avoid overparametrization. Moreover, the intermolecular magnetic coupling ( $zJ'$ ) and the  $D$  parameter are very closely related and their independent contributions cannot be easily accounted for. This result indicates that, besides the intramolecular coupling, the zero field splitting and the intermolecular coupling

are present but their correct evaluation is not possible given their close relation as was also found in various Ni(II) complexes.<sup>2c,d</sup>

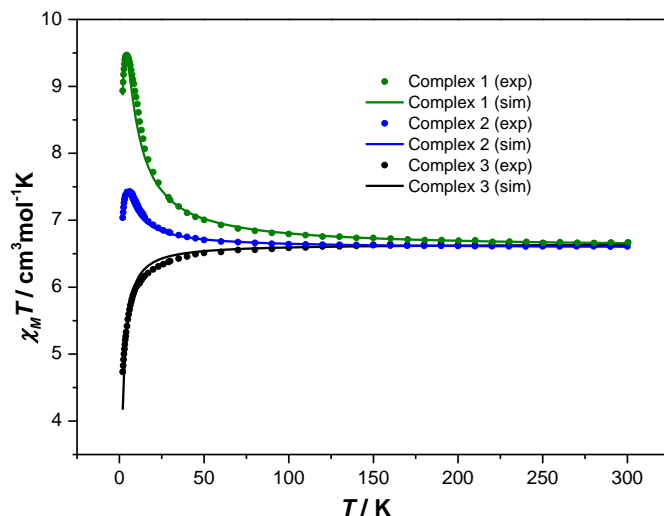


**Figure 5.** Thermal dependence of the  $\chi_M T$  for complexes **1-3**. Symbols represent experimental data while straight lines represent the simulations obtained from the parameters indicated in the main text.

**Discussion.** In all complexes, Ni<sup>II</sup> and Mn<sup>II</sup> centers are linked through two monodentate oxygen atoms coming from the deprotonation of two phenol groups that belong to the same ligand L and simultaneously by a bidentate carboxylate group coordinated to the metal ions in a *syn-syn* mode. One of the parameters that has been observed to have a crucial effect on the magnetic coupling between ions is the M-O-M' angle from the monodentate bridge, being M and M' the same or different metallic ions. There seems to be a critical value of the angle above which the superexchange is antiferromagnetic and below which the interaction becomes ferromagnetic, and this is called critical angle. Actually, the critical angle has been very accurately determined for  $\mu_2$ -phenoxido-bridged Cu<sup>II</sup> homonuclear compounds.<sup>1a</sup> However, there is still a lack of empirical information of the effect of this angle in coordination complexes other than those based on Cu<sup>II</sup> ions, not to mention in the heteropolynuclear compounds. Nevertheless there is the possibility that other metallic ions or the combination of different metallic ions with a similar M-O-M' skeleton might *push* this angle to higher values in order to obtain ferromagnetic complexes with a larger variety of geometries. In fact, and keeping this in mind, we decided to compare the value of this angle for the very limited amount of  $\mu_2$ -phenoxido-bridged Ni<sub>2</sub>Mn compounds reported so

far that might also present *syn-syn* carboxylate bridges to fulfill the coordination sphere of their paramagnetic ions, hence they are easily comparable in all terms. *Syn-syn* carboxylate bridges have often been observed to lead to antiferromagnetic interactions in homonuclear complexes.<sup>33</sup> However, the heterometallic nature of the complexes studied in this work can effectively weaken such antiferromagnetic exchange, as explained later, and thus it has not been considered for simplicity. Table 3 shows the main structural features of those compounds including the ones reported in this work, ordered by decreasing value of the magnetic exchange constant obtained from either the fit or the simulation of the experimental data.

**Table 3.** Selected structural parameters of  $\mu_2$ -phenoxido-bridged  $\text{Ni}_2\text{Mn}$  complexes, ordered by decreasing value of the magnetic exchange constant.

Compound		$J_{\text{Ni-Mn}} \text{ exp./}$ $\text{cm}^{-1}$	$J_{\text{Ni-Mn}} \text{ calc./}$ $\text{cm}^{-1}$	Num. of $\mu_2$ - pheno xido- bridges	Ni-O-Mn Angle / °	Ref.
$[\text{Mn}^{\text{II}}(\text{Ni}^{\text{II}}\text{L})_2] \cdot 2\text{CH}_3\text{OH}$		+9.30	+8.3 (-0.3)	3	86.38	8
Complex <b>1</b> *	av.	+1.38	+1.0	2	97.24	This work
	1		+1.2 (-0.3)	2	96.89	
	2		+0.8 (-0.3)	2	97.61	
Complex <b>2</b> *	av.	+0.50	+0.25	2	96.43	This work
	1		-0.4 (-0.3)	2	95.87	
	2		+0.9 (-0.3)	2	96.99	
Complex <b>3</b>		-0.24	-1.4 (-0.2)	2	98.51	This work
$[\text{Mn}^{\text{II}}(\text{Ni}^{\text{II}}\text{L})_2(\text{OAc})_4(\text{H}_2\text{O})_2]$		-0.30	-3.4 (-0.1)	1	102.31	7

\* two non-equivalent molecules in the unit cell

As can be seen from Table 3, the number of  $\mu_2$ -phenoxido-bridges between the  $\text{Ni}^{\text{II}}$  and  $\text{Mn}^{\text{II}}$  centers is directly correlated to the Ni-O-Mn angle, being  $86.38^\circ$  the lowest in the case there are three bridges, and  $102.31^\circ$  the largest when only one phenoxide is bridging the magnetic ions. Our complexes, in which the two ions are linked by two monodentate phenoxide bridges, show very similar angles with an average value of  $97.24^\circ$  for **1**,  $96.43^\circ$  for **2** and  $98.51^\circ$  for **3** being these three values in between of those previously mentioned. Concerning the value of the magnetic exchange constant ( $J_{\text{Ni-Mn}}$ ), this seems to follow exactly the same trend by which low values of the angle derive in ferromagnetic coupling while the largest ones induce the antiferromagnetic exchange. A linear fit showing a possible dependence of the magnetic exchange constant  $J_{\text{Ni-Mn}}$  with the Ni-O-Mn angle is shown in Figure 6. The fit with an adjusted- $R^2$  of 0.88 indicates that the critical angle for  $\mu_2$ -phenoxido-bridged  $\text{Ni}^{\text{II}}$ - $\text{Mn}^{\text{II}}$  complexes could be around  $99^\circ$ .

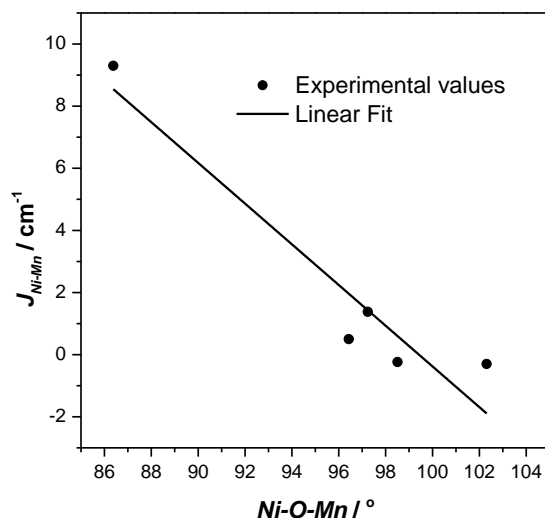


**Figure 6.** Variation of the magnetic coupling ( $J_{\text{Ni-Mn}}$ ) in trinuclear  $\text{Ni}_2\text{Mn}$  double phenoxido-bridged complexes with the average Ni-O-Mn bond angle. Data are extracted from complexes **1-3** of the present work and from complex **1** of reference 8 and complex **2** of reference 7.

However, complex **2** shows the lowest Ni-O-Mn angle among the complexes reported in this work and thus the strongest ferromagnetic exchange is expected for complex **2** compared to complexes **1** and **3**. Nevertheless, complex **2** shows an intermediate  $J_{\text{Ni-Mn}}$ , lower than the one of complex **1**. The crystal structure of complex **2** shows two non-equivalent molecules in the

structure from which one of them presents a coordination number of five for its two  $\text{Ni}^{\text{II}}$  ions, as opposed to all other  $\text{Ni}^{\text{II}}$  centers in complexes **1-3** where they are six-coordinated. This fact strongly affects the  $\text{Ni}^{\text{II}}\text{-Mn}^{\text{II}}$  magnetic exchange interaction in this complex and it is the reason for such disagreement in the magnetostructural correlation as it will be shown later by means of theoretical calculations. The critical angles for five different families of  $\mu_2$ -phenoxido-bridged M-M' polynuclear compounds have been depicted in Figure 7, where the critical angle is defined as the M-O-M' angle formed by the monodentate phenoxido-based bridging ligand. While for homometallic polynuclear complexes of either  $\text{Cu}^{\text{II}}$ ,  $\text{Ni}^{\text{II}}$  or  $\text{Mn}^{\text{III}}$  ions, these values have been extracted or assigned from the results reported in the literature by other authors,<sup>1a,3d,e,34</sup> the values of the critical angles associated to heterometallic polynuclear complexes like  $\text{Ni}^{\text{II}}\text{-Mn}^{\text{II}}$  and  $\text{Cu}^{\text{II}}\text{-Mn}^{\text{II}}$  systems, have been tentatively assigned based on correlations established with Schiff base trinuclear complexes studied by us in this work and in reference<sup>6e</sup> respectively. Apparently, among the five different families of polynuclear compounds compared, the heterometallic one based on  $\text{Cu}^{\text{II}}\text{-Mn}^{\text{II}}$  ions shows the lowest critical angle of all, restricting the range of angles that lead to ferromagnetic exchange as compared to more established homometallic compounds made of  $\text{Cu}^{\text{II}}$ ,  $\text{Ni}^{\text{II}}$  or  $\text{Mn}^{\text{III}}$  ions. On the other hand, the family of heterometallic complexes based on  $\text{Ni}^{\text{II}}\text{-Mn}^{\text{II}}$  ions could represent an increase of this value up to ca.  $99^\circ$ , comparable to the value reported for  $\mu_2$ -phenoxido-bridged  $\text{Mn}^{\text{III}}$ -based homometallic complexes and significantly higher than the one reported for analogous  $\text{Ni}^{\text{II}}$ -based homometallic complexes. Still,  $\text{Mn}(\text{III})$ -based homometallic complexes show the highest critical angle at  $101^\circ$ <sup>3d,e</sup> thus remaining as the family of  $\mu_2$ -phenoxido-bridged polynuclear complexes with the largest range of angles available for ferromagnetic exchange. Despite this, similar heterometallic compounds based on  $\text{Mn}^{\text{III}}$  ions have been rarely studied from this point of view and definitely deserve more attention due to the potential they hold.



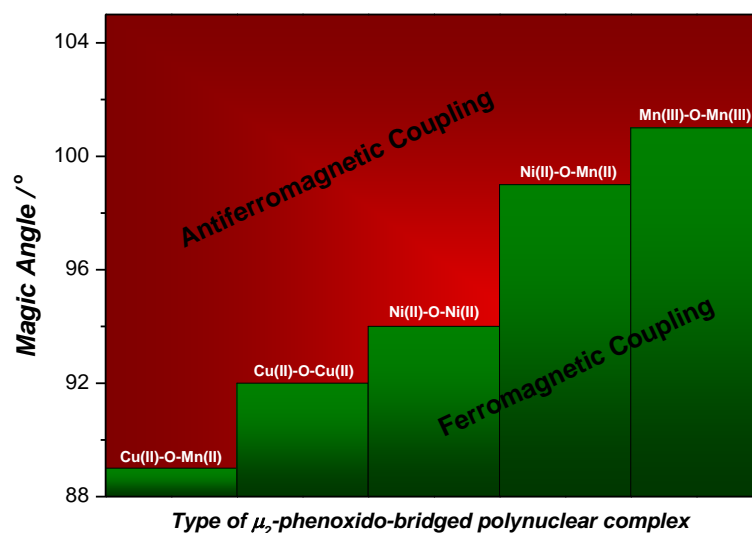


**Figure 7.** Critical angles for five different families of  $\mu_2$ -phenoxido-bridged M-M' polynuclear compounds. For homometallic polynuclear complexes, these values have been extracted from references 1a, 3d,e, 33. The values of the critical angles associated to heterometallic polynuclear complexes have been tentatively assigned based on correlations established in this work and in reference 6e.

**Theoretical Results.** The calculated exchange coupling constants (see Computational details section) of the three synthesized  $\text{Ni}_2\text{Mn}$  complexes (**1-3**) together with those of two systems previously reported are collected in Table 3 and depicted in Figure 8.<sup>7,8</sup> As shown in Figure 8 there is a clear magnetostructural correlation between the Ni-O-Mn angle and the  $J_{\text{Ni-Mn}}$  values, in agreement with what was observed experimentally (Figure 6). The coordination number of the  $\text{Ni}^{\text{II}}$  cations is six with the exception of one of the molecules of complex **2** (black circle in Figure 8 and antiferromagnetic coupling of  $-0.4 \text{ cm}^{-1}$  in Table 3). However, the inclusion of a methanol molecule in this structure to reach the coordination six present in all the other cases results in a ferromagnetic coupling of  $+2.2 \text{ cm}^{-1}$  (white circle in Figure 8) improving the magnetostructural correlation expressed by a linear regression with an adjusted- $R^2$  of 0.97. The calculation of next-nearest neighbour  $J_{\text{Ni-Ni}}$  constants shows that in all cases correspond to weak antiferromagnetic couplings. Furthermore, these  $J_{\text{Ni-Ni}}$  values become slightly less antiferromagnetic when increasing the Ni-O-Mn angle, just the opposite behaviour of the  $J_{\text{Ni-Mn}}$  couplings.

As pointed out in Figure 7, the interaction between Ni<sup>II</sup> and Mn<sup>II</sup> centers needs a relatively large Ni-O-Mn critical angle to become antiferromagnetic. In order to justify this fact, we can apply a simple rule based on the Kahn-Briat model.<sup>35-37</sup> By considering the number and symmetry of interactions of pairs of magnetic orbitals for the Ni<sup>II</sup>-Mn<sup>II</sup> systems, we can expect respectively 2 antiferromagnetic and 8 ferromagnetic contributions. For instance, only one of the five d orbitals of Mn<sup>II</sup> will have the right symmetry to give an antiferromagnetic contribution in its interaction with each one of the two orbitals bearing the unpaired electrons of the Ni<sup>II</sup> center. Due to the relatively high number of the ferromagnetic contributions, the Ni<sup>II</sup>-Mn<sup>II</sup> systems have a large tendency to show ferromagnetic coupling and only large Ni-O-Mn angles (above 98°) can induce antiferromagnetism.

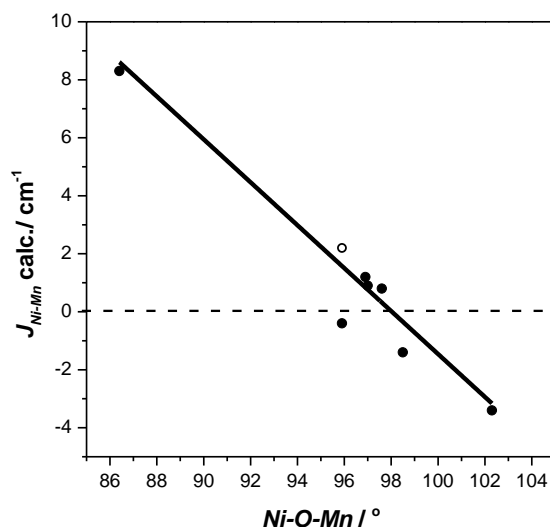


**Figure 8.** Dependence between the calculated  $J_{Ni-Mn}$  values and the average Ni-O-Mn angle of the  $\mu_2$ -phenoxido bridging ligands. For molecule **1** of complex **2**, with a Ni-O-Mn angle of 95.87°, an antiferromagnetic coupling with  $J_{Ni-Mn} = -0.4$  cm<sup>-1</sup> was found experimentally (black circle) since Ni<sup>II</sup> centers are five-coordinated. A  $J_{Ni-Mn}$  value of +2.2 cm<sup>-1</sup> is calculated (white circle) by adding a methanol molecule to have the same coordination than the other systems.

The calculated spin density distribution for the ground state of complex **1** showing ferromagnetic coupling between Ni<sup>II</sup> and Mn<sup>II</sup> centers (see Table 3) is represented in Figure 9. As expected, due to the d<sup>5</sup> electronic configuration of the Mn<sup>II</sup> cation, the spin distribution is almost spherical

while in the  $\text{Ni}^{\text{II}}$  centers is the square of the sum of the  $d_z^2$  and  $d_{x^2-y^2}$  magnetic orbitals. Due to the presence of unpaired electrons in all the antibonding metal-ligand orbitals (those of  $t_{2g}$  symmetry assuming  $O_h$  symmetry), there is a predominance of the spin delocalization due to the strong mixing of metal-ligand orbitals.<sup>38,39</sup> This fact results in that all the atoms coordinated to the metals have the same sign of spin population. Small white lobes in some of the carbon atoms of the terminal ligands indicate that the spin polarization mechanism prevails in the atoms of the second coordination sphere.

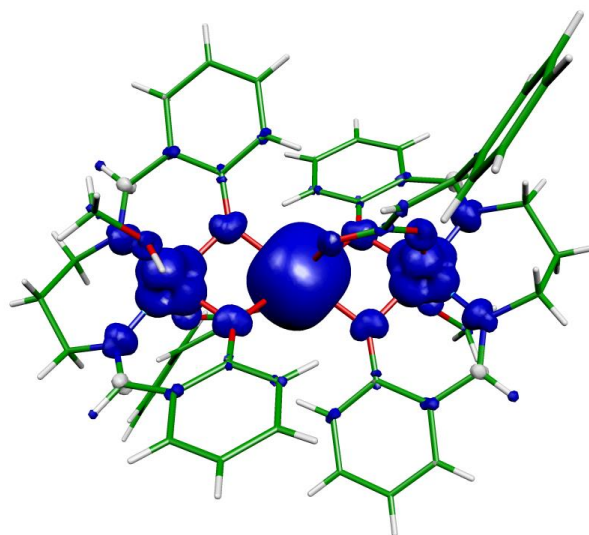


**Figure 9.** Spin density distribution for complex **1** corresponding to the  $S = 9/2$  ground state. The isodensity surface represented corresponds to a value of  $0.005 \text{ e}^-/\text{bohr}^3$  (positive and negative values are represented as blue and white surfaces, respectively).

## Conclusions

Three new  $\text{Ni}^{\text{II}}\text{--Mn}^{\text{II}}$  complexes derived from a salen type Schiff base ligand along with various *syn-syn* bridging carboxylate coligands viz. cinnamate, phenylacetate and salicylate have been synthesized and characterized in order to determine the crossover angle experimentally. All three have similar trinuclear structure comprising of a central octahedral  $\text{Mn}^{\text{II}}$  and two terminal octahedral or square pyramidal  $\text{Ni}^{\text{II}}$  having slight variation in Ni-O-Mn angle ( $96.43\text{--}98.51^\circ$ ). A linear dependency was found in these  $\text{Ni}^{\text{II}}\text{--Mn}^{\text{II}}$  diphenoxido-bridged complexes between the  $J_{\text{Ni-Mn}}$  value and the Ni-O-Mn angle of the monodentate phenoxido bridges, from which a high value

of the crossover angle from ferro to antiferromagnetic exchange could be assigned. This value corresponds approximately to  $98^\circ$  and apparently indicates that the family of  $\text{Ni}^{\text{II}}\text{--Mn}^{\text{II}}$  complexes is the one that supports ferromagnetic interactions for a higher angle among the various known MM' diphenoxido-bridged complexes, with the exception of the  $\text{Mn}^{\text{III}}\text{Mn}^{\text{III}}$  compounds. Theoretical calculations also indicate that an incomplete octahedral coordination sphere for these ions can significantly alter this correlation, and thus it is only valid for six-coordinated species.

## Acknowledgements

We thank DST-FIST, India funded Single Crystal Diffractometer Facility at the Department of Chemistry, University of Calcutta, Kolkata, India. The authors thank Department of Science and Technology (DST), New Delhi, India, for financial support (SR/S1/IC/0034/2012). P.S is thankful to UGC for research fellowship [UGC/52/Jr. Fellow (Enhancement) dated 17.01.2013]. A.F acknowledges financial support from the Spanish MINECO through CTQ2012-32247 and for a Ramón y Cajal Fellowship (RYC-2010-05821). J.J and E.R. thank the Spanish Ministerio de Economía y Competitividad (CTQ2011-23862-C02-01) and the regional Generalitat de Catalunya authority (2009SGR-1459). The authors thankfully acknowledge the computer resources, technical expertise and assistance provided by the CESCA.

## References

1. a) Yazigia, D. V.; Aravenab, D.; Spodineb, E.; Ruiz, E.; Alvarez, S. *Coord. Chem. Rev.* **2010**, 254, 2086–2095 and references therein; b) Biswas, C.; Drew, M. G. B.; Ruiz, E. Estrader, M.; Diaz, C.; Ghosh, A. *Dalton Trans.* **2010**, 39, 7474–7484; c) Ding, C.; Gao, C.; Ng, S.; Wang, B.; Xie, Y.; *Chem. Eur. J.* **2013**, 19, 9961 – 9972; d) Ray, A.; Mitra, S.; Khalaji, A. D.; Atmani, C.; Cosquer, N.; Triki, S.; Juan, J. M. C.; Serra, S. C.; Gómez-García, C. J.; Butcher, R. J.; Garribba, E.; Xuh, D.; *Inorganica Chimica Acta* **2010**, 363, 3580–3588.
2. a) Biswas, R.; Kar, P.; Song, Y.; Ghosh, A. *Dalton Trans.* **2011**, 40, 5324–5331; b) Nanda, K. K.; Das, R.; Thompson, L. K.; Venkatsubramanian, K.; Nag, K.; *Inorg. Chem.* **1994**, 33, 1188–1193; c) Mukherjee, P.; Drew, M. G. B.; Gomez-García, C. J.; Ghosh, A.; *Inorg. Chem.*

- 2009**, 48, 5848-5860; d) Mukherjee, P.; Drew, M. G. B.; Tangoulis, V.; Estrader, M.; Diaz, C.; Ghosh, A.; *Polyhedron* **2009**, 28, 2989–2996.
3. a) Chumillas, M. V.; Tanase, S.; Mutikainen, I.; Turpeinen, U.; Jongh, L. J. de; Reedijk, J.; *Inorg. Chem.* **2008**, 47, 5919-5929 ; b) Watkinson, M.; Fondo, M.; Bermejo, M. R.; Sousa, A.; McAuliffe, C. A.; Pritchard, R. G.; Jaiboon, N.; Aurangzeb, N.; Naeem, M. *J. Chem. Soc., Dalton Trans.* **1999**, 31-42 ; c) Sailaja, S.; Reddy, K. R.; Rajasekharan, M. V.; Hureau, C.; Riviere, E.; Cano, J.; Girerd, J.-J. *Inorg. Chem.* **2003**, 42, 180-186; d) Lu, Z.; Yuan, M.; Pan, F.; Gao, S.; Zhang, D.; Zhu, D. *Inorg. Chem.* **2006**, 45, 3538-3548; e) Bhargavi, G.; Rajasekharan, M. V.; Costes, J.-P.; Tuchagues, J.-P. *Polyhedron* **2009**, 28, 1253-1260.
  4. a) Ruiz, E.; Alemany, P.; Alvarez, S.; Cano, J. *Inorg. Chem.* **1997**, 36, 3683-3688; b) Burkhardt, A.; Spielberg, E. T.; Simon, S.; Gçrls, H.; Buchholz, A.; Plass, W. *Chem.–Eur. J.* **2009**, 15, 1261-1271.
  5. a) Biswas, S.; Ghosh; A. *Polyhedron* **2013**, 65, 322–331; b) Biswas, S.; Diaz, C.; Ghosh, A. *Polyhedron* **2013**, 51, 96–101; c) Tao, R.-J.; Mei, C.-Z.; Zang, S.-Q.; Wang, Q.-L.; Niu, J.-Y.; Liao, D.-Z. *Inorg. Chim. Acta* **2004**, 357, 1985-1990; d) Journaux, Y.; Khan, O.; Badarau, I. M.; Galy, J.; Jaud, J.; Bencini, A.; Gatteschi, D. *J. Am. Chem. Soc.* **1985**, 107, 6305-6312.
  6. a) Biswas, S.; Naiya, S.; Gómez-García, C. J.; Ghosh, A. *Dalton Trans.* **2012**, 41, 462-473; b) Mei; C.Z., Tao, R.-J.; Wang, Q.-L. *Acta Chim. Sinica.* **2007**, 65, 1129-1134; c) Brychey, K.; Jens, K.-J.; Tilset, M.; Behrens, U. *Chem. Ber.* **1994**, 127, 991-995 ; d) Öz, S.; Kurtaran, R.; Arici, C.; Ergun, Ü.; Kaya, F. N. D.; Emregül, K. C.; Atakol, O.; Ülkü, D. *J. Therm. Anal. Calorim.* **2010**, 99, 363-368; e) Seth, P.; Ghosh, S.; Figuerola, A.; Ghosh, A. *Dalton Trans.* **2014**, 43, 990-998.
  7. Sharma, A. K.; Lloret, F.; Mukherjee, R. *Inorg. Chem.* **2007**, 46, 5128-5130.
  8. Kobayashi, T.; Yamaguchi, T.; Ohta, H.; Sunatsuki, Y.; Kojima, M.; Re, N.; Nonoyama, M.; Matsumoto, N.; *Chem. Commun.* **2006**, 1950-1952.

9. a) Sari, M.; Atakol, O.; Svoboda, I. *Anal.Sci.:X-Ray Struct.Anal.Online* **2005**, *21*, x205-x206;  
b) Ercan, F.; Atakol, O. *Acta Crystallogr.,Sect.C:Cryst.Struct.Commun.* **1998**, *54*,1268-1270;  
c) Ercan, F.; Atakol, O.; Arici, C.; Svoboda, I.; Fuess, H. *Acta Crystallogr., Sect.C:Cryst.Struct.Commun.* **2002**, *58*, m193-m196; d) Atakol, O.; Nazir, H.; Durmus, Z.; Svoboda, I.; Fuess H. *Anal.Sci.* **2002**, *18*, 493; e) Chen, H.; Ma, C. B.; Yuan, D. Q.; Hu, M.-Q.; Wen, H.-M.; Liu, Q.-T; Chen, C.-N. *Inorg.Chem.* **2011**, *50*, 10342-10352.
10. a) Biswas, S.; Naiya, S.; Drew, M. G. B.; Estarellas, C.; Frontera, A.; Ghosh, A.; *Inorg. Chim. Acta*, **2011**, *366*, 219-226; b) Das, L. K.; Park, S.-W.; Choc, S. J.; Ghosh, A. *Dalton Trans.* **2012**, *41*, 11009-11017; c) Ghosh, A. K.; Bauzá, A.; Bertolasi, V.; Frontera, A.; Ray, D. *Polyhedron* **2013**, *53*, 32-39.
11. Reglinski, J.; Morris, S.; Stevenson, D. E. *Polyhedron* **2002**, *21*, 2167–2174.
12. Drew, M. G. B.; Prasad, R. N.; Sharma, R. P. *Acta Crystallogr. Sect. C: Cryst. Struct. Commun.* **1985**, *41*, 1755–1758.
13. Ruiz, E.; Alemany, P.; Alvarez, S.; Cano, J. *J. Am. Chem. Soc.* **1997**, *119*, 1297-1303.
14. Ruiz, E. *Struct. Bond.* **2004**, *113*, 71.
15. Ruiz, E.; Rodríguez-Forteza, A.; Cano, J.; Alvarez, S.; Alemany, P. *J. Comp. Chem.* **2003**, *24*, 982-989.
16. Ruiz, E.; Alvarez, S.; Cano, J.; Polo, V. *J. Chem. Phys.* **2005**, *123*, 164110.
17. Ruiz, E.; Forteza, A. R.; Tercero, J.; Cauchy, T.; Massobrio, C. *J. Chem. Phys.* **2005**, *123*, 074102.
18. Becke, A. D. *J. Chem. Phys.* **1993**, *98*, 5648–5652.
19. Gaussian 09 (Revision D01): Frisch, M. J.; Trucks, G. W.; Schlegel, H. B.; Scuseria, G. E.; Robb, M. A.; Cheeseman, J. R.; Scalmani, G.; Barone, V.; Mennucci, B.; Petersson, G. A.; Nakatsuji, H.; Caricato, M.; Li, X.; Hratchian, H. P.; zmaylov, A. F.; Bloino, I. J.; Zheng, G.; Sonnenberg, J. L.; Hada, M.; Ehara, M.; Toyota, K.; Fukuda, R.; Hasegawa, J.; Ishida, M.; Nakajima, T.; Honda, Y.; Kitao, O.; Nakai, H.; Vreven, T.; Montgomery, J. J. A.; Peralta, J.

- E.; Ogliaro, F.; Bearpark, M.; Heyd, J. J.; Brothers, E.; Kudin, K. N.; Staroverov, V. N.; Kobayashi, R.; Normand, J.; Raghavachari, K.; Rendell, A.; Burant, J. C.; Iyengar, S. S.; Tomasi, J.; Cossi, M.; Rega, N.; Millam, J. M.; Klene, M.; Knox, J. E.; Cross, J. B.; Bakken, V.; Adamo, C.; Jaramillo, J.; Gomperts, R.; Stratmann, R. E.; Yazyev, O.; Austin, A. J.; Cammi, C.; Pomelli, J.W.; Ochterski, R.; Martin, R. L.; Morokuma, K.; Zakrzewski, V. G.; Voth, G. A.; Salvador, P.; Dannenberg, J. J.; Dapprich, S.; Daniels, A. D.; Farkas, O.; Foresman, J. B.; Ortiz, J.V.; Cioslowski, J.; Fox, D. J. Wallingford, CT, **2009**.
20. Jaguar 7.0: Schrödinger, LLC, New York, **2007**.
  21. Vacek, G.; Perry, J. K.; Langlois, J.-M. *Chem. Phys. Lett.* **1999**, *310*, 189–194.
  22. Schaefer, A.; Huber, C.; Ahlrichs, R. *J. Chem. Phys.* **1994**, *100*, 5829–5835.
  23. SAINT, version 6.02, SADABS, version 2.03, Bruker AXS, Inc., Madison, WI, 2002.
  24. Sheldrick, G. M. SHELXS-97, Program for solution of crystal structures, University of Göttingen, Germany, 1997.
  25. Sheldrick, G. M. SHELXL-97, Program for refinement of crystal structures, University of Göttingen, Germany, 1997.
  26. Spek, A. L. *Acta Crystallogr., Sect. A: Fundam. Crystallogr.* **1990**, *46*, C34.
  27. Farrugia, L. J. *J. Appl. Crystallogr.* **1997**, *30*, 565.
  28. Farrugia, L. J. *J. Appl. Crystallogr.* **1999**, *32*, 837.
  29. Addison, A.W.; Rao, T. N.; Reedjik, J.; Rijn, J. V.; Verschoor, C. G.; *J. Chem. Soc., Dalton Trans.* **1984**, 1349-1356.
  30. a) Seth, P.; Das, L. K.; Drew, M. G. B.; Ghosh, A. *Eur. J. Inorg. Chem.* **2012**, 2232–2242; b) Das, L. K.; Drew, M. G. B.; Ghosh, A. *Inorg. Chim. Acta* **2013**, *394*, 247–254; c) Das, L. K.; Biswas, A.; Gómez-García, C. J.; Drew, M. G. B.; Ghosh, A. *Inorg. Chem.* **2014**, *53*, 434–445.
  31. Yang, L.; Powell, D. R.; Houser, R. P.; *Dalton Trans.* **2007**, 955-964.

32. a) Almenar, J. J. B.; Juan, J. M. C.; Coronado, E.; Tsukerblat, B. S. *J. Comput. Chem.* **2001**, 22, 985-991; b) Almenar, J. J. B.; Juan, J. M. C.; Coronado, E.; Tsukerblat, B. S.; *Inorg. Chem.* **1999**, 38, 6081-6088.
33. Ghoshal, D.; Maji, T. K.; Mostafa, G.; Sain, S.; Lu, T.-H.; Ribas, J.; Zangrando, E.; Chaudhuri, N. R. *Dalton Trans.* **2004**, 1687-1695.
34. a) Bu, X.-H.; Du, M.; Zhang, L.; Liao, D.-Z.; Tang, J.-K.; Zhang, R.-H.; Shionoya, M.; *J. Chem. Soc., Dalton Trans.* **2001**, 593-598; b) Biswas, R.; Giri, S.; Saha, S. K.; Ghosh, A. *Eur. J. Inorg. Chem.* **2012**, 2916-2927.
35. Kahn, O.; Briat, B., *J. Chem. Soc. Trans.* **1976**, 72, 268-281.
36. Kahn, O.; Briat, B., *J. Chem. Soc. Trans.* **1976**, 72, 1441-1446.
37. Kahn, O., *Molecular Magnetism. VCH Publishers: New York* **1993**.
38. Ruiz, E.; Cirera, J.; Alvarez, S., *Coord. Chem. Rev.* **2005**, 249, 2649-2660.
39. Cano, J.; Ruiz, E.; Alvarez, S.; Verdaguer, M., *Comments on Inorg. Chem.* **1998**, 20, 27-56.



**Table 1.** Crystal data and structure refinement of complexes **1-3**:

	<b>1</b>	<b>2</b>	<b>3</b>
Formula	C <sub>56</sub> H <sub>61</sub> N <sub>4</sub> O <sub>12</sub> Ni <sub>2</sub> Mn	C <sub>51</sub> H <sub>50</sub> N <sub>4</sub> O <sub>10</sub> Ni <sub>2</sub> Mn	C <sub>84</sub> H <sub>82</sub> N <sub>8</sub> O <sub>16</sub> Ni <sub>4</sub> Mn
Formula weight	1154.41	1051.26	1749.28
Space group	P -1	P -1	P -1
Crystal system	Triclinic	Triclinic	Triclinic
<i>a</i> / Å	10.8407(9)	9.3692(13)	12.004(5)
<i>b</i> / Å	14.1770(12)	10.5173(14)	12.166(5)
<i>c</i> / Å	18.5894(16)	23.878(3)	14.238(5)
$\alpha$ /°	90.611(4)	90.311(2)	89.107(5)
$\beta$ /°	92.259(4)	99.130(2)	69.512(5)
$\gamma$ /°	104.275(3)	90.807(2)	88.037(5)
<i>V</i> /Å <sup>3</sup>	2766.0(4)	2322.8(5)	1946.6(13)
<i>Z</i>	2	2	1
Calculated density <i>D</i> <sub>cal</sub> /g cm <sup>-3</sup>	1.386	1.503	1.492
Absorption coeff.( $\mu$ ) mm <sup>-1</sup>	(MoK $\alpha$ ) 0.962	(MoK $\alpha$ ) 1.135	(MoK $\alpha$ ) 1.181
<i>F</i> (000)	1204.0	1090.0	907
R(int)	0.030	0.021	0.025
$\theta$ range (deg)	1.1 to 28.4	0.9 to 26.4	1.5 to 26.5
Total reflections	35517	17569	24251
Unique reflections	13444	8940	7783
<i>I</i> >2 $\sigma$ ( <i>I</i> )	10683	7044	6454
R1, wR2	0.0438, 0.1341	0.0413, 0.1104	0.0358, 0.1031
Temp (K)	293	293	293

**Table 2.** Dimensions in the metal coordination spheres in **1A**, **1B**, **2A**, **2B** and **3A**, **3B** (distances, Å, angles, °).

	<b>1A</b>	<b>2A</b>	<b>3A</b>
Ni(1)-O(1)	2.028(2)	2.016(2)	2.016(2)
Ni(1) -O(2)	2.023(2)	2.022(2)	2.006(2)
Ni(1) -O(3)	2.055(2)	2.054(3)	2.095(2)
Ni(1) -O(5)	2.153(2)	2.153(3)	2.185(2)
Ni(1) -N(1)	2.024(2)	2.021(3)	2.037(2)
Ni(1) -N(2)	2.035(2)	2.016(3)	2.042(2)
Mn(1) -O(2)	2.170(2)	2.175(2)	2.171(2)
Mn(1) -O(4)	2.210(2)	2.199(2)	2.185(2)
Mn(1) -O(1)	2.158(2)	2.158(2)	2.174(2)
Mn(1) -O(4) <sup>a</sup>	2.210(2)	2.199(2)	2.185(2)
Mn(1) -O(1) <sup>a</sup>	2.151(2)	2.158(2)	2.174(2)
Mn(1) -O(2) <sup>a</sup>	2.170(2)	2.175(2)	2.171(2)
O(1)-Ni(1)-O(2)	82.31(7)	83.30(8)	80.04(6)
O(1)-Ni(1)-O(3)	92.50(7)	91.61(8)	91.40(7)
O(1)-Ni(1)-O(5)	88.99(8)	87.55(10)	91.51(7)
O(1)-Ni(1)-N(1)	90.59(8)	90.70(11)	90.78(7)
O(1)-Ni(1)-N(2)	173.18(8)	172.45(11)	170.18(8)
O(2)-Ni(1)-O(3)	94.05(7)	95.22(9)	95.05(7)
O(2)-Ni(1)-O(5)	88.07(10)	89.63(9)	89.53(8)
O(2)-Ni(1)-N(1)	172.82(8)	173.73(11)	170.70(7)
O(2)-Ni(1)-N(2)	91.03(8)	89.58(11)	90.42(8)
O(3)-Ni(1)-O(5)	177.56(10)	174.95(10)	174.94(8)
O(3)-Ni(1)-N(1)	87.28(8)	86.75(13)	86.59(8)
O(3)-Ni(1)-N(2)	89.44(8)	91.52(10)	87.13(7)
O(5)-Ni(1)-N(1)	90.77(11)	88.29(13)	89.23(9)
O(5)-Ni(1)-N(2)	89.30(9)	89.93(12)	90.70(8)
N(1)-Ni(1)-N(2)	96.04(9)	96.33(13)	98.82(9)
O(2)-Mn(1)-O(4) <sup>a</sup>	92.15(7)	92.77(7)	90.04(6)
O(4)-Mn(1)-O(4) <sup>a</sup>	180.00	180.00	180.00
O(1) <sup>a</sup> -Mn(1)-O(2) <sup>a</sup>	76.19(6)	76.53(7)	73.08(6)
O(1) <sup>a</sup> -Mn(1)-O(4) <sup>a</sup>	86.29(7)	85.62(7)	90.73(7)
O(2) <sup>a</sup> -Mn(1)-O(4) <sup>a</sup>	87.85(7)	87.23(7)	89.97(6)
O(1)-Mn(1)-O(4) <sup>a</sup>	93.71(7)	94.38(7)	89.27(7)
O(1) <sup>a</sup> -Mn(1)-O(4)	93.71(7)	94.38(7)	89.27(7)
O(2) <sup>a</sup> -Mn(1)-O(4)	92.15(7)	92.77(7)	90.04(6)
O(1)-Mn(1)-O(2)	76.19(6)	76.53(7)	73.08(6)
O(1)-Mn(1)-O(4)	86.29(7)	85.62(7)	90.73(7)
O(1)-Mn(1)-O(1) <sup>a</sup>	180.00	180.00	180.00

O(1)-Mn(1)-O(2) <sup>a</sup>	103.81(6)	103.47(7)	106.92(6)
O(2)-Mn(1)-O(2) <sup>a</sup>	180.00	180.00	180.00
O(2)-Mn(1)-O(4)	87.85(7)	87.23(7)	89.97(6)
O(1) <sup>a</sup> -Mn(1)-O(2)	103.81(6)	103.47(7)	106.92(6)
Ni(1)-O(1)-Mn(1)	97.74(7)	97.34(8)	98.31(7)
Ni(1)-O(2)-Mn(1)	97.29(7)	96.58(8)	98.70(7)

<sup>a</sup> represents symmetry element 2-x,-y,-z in **1A**, -x,-3-y,-3-z in **2A**, 2-x,1-y,2-z in **3A**.

	<b>1B</b>	<b>2B</b>	<b>3B</b>
Ni(2)-O(6)	2.017(2)	2.002(2)	1.845(3)
Ni(2)-O(7)	2.020(2)	1.999(2)	1.862(2)
Ni(2)-N(3)	2.030(2)	2.017(2)	1.889(3)
Ni(2)-N(4)	2.022(2)	2.014(2)	1.900(5)
Ni(2)-O(9)	2.052(2)	1.995(2)	
Ni(2)-O(10)	2.147(3)		
Mn(2)-O(6)	2.212(2)	2.161(2)	
Mn(2)-O(6) <sup>b</sup>	2.212(2)	2.161(2)	
Mn(2)-O(7)	2.120(2)	2.163(2)	
Mn(2)-O(7) <sup>b</sup>	2.120(2)	2.163(2)	
Mn(2)-O(8)	2.225(2)	2.138(2)	
Mn(2)-O(8) <sup>b</sup>	2.225(2)	2.138(2)	
N(3)-Ni(2)-N(4)	97.25(9)	95.50(9)	94.16(14)
O(7)-Ni(2)-N(4)	89.76(9)	89.68(8)	92.36(12)
O(7)-Ni(2)-N(3)	172.74(8)	165.00(8)	168.91(11)
O(6)-Ni(2)-O(7)	82.14(7)	81.91(8)	80.89(10)
O(6)-Ni(2)-N(3)	90.91(8)	88.84(8)	93.86(13)
O(6)-Ni(2)-N(4)	171.72(8)	160.97(8)	169.27(13)
O(7)-Ni(2)-O(9)	94.77(8)	100.08(8)	
O(9)-Ni(2)-N(3)	87.64(8)	93.28(8)	
O(9)-Ni(2)-N(4)	86.08(9)	96.92(9)	
O(6)-Ni(2)-O(9)	92.90(7)	101.33(8)	
O(6)-Ni(2)-O(10)	89.53(10)		
O(7)-Ni(2)-O(10)	89.01(9)		
O(9)-Ni(2)-O(10)	175.75(9)		
O(10)-Ni(2)-N(3)	88.84(10)		
O(10)-Ni(2)-N(4)	92.01(11)		
O(7)-Mn(2)-O(7) <sup>b</sup>	180.00	180.00	
O(6)-Mn(2)-O(7)	75.48(7)	74.65(7)	
O(6)-Mn(2)-O(8)	91.84(7)	86.74(7)	
O(6)-Mn(2)-O(6) <sup>b</sup>	180.00	180.00	
O(6)-Mn(2)-O(7) <sup>b</sup>	104.52(7)	105.35(7)	

O(6)-Mn(2)-O(8) <sup>b</sup>	88.16(7)	93.26(7)	
O(7)-Mn(2)-O(8) <sup>b</sup>	93.66(7)	93.37(7)	
O(6) <sup>b</sup> -Mn(2)-O(8)	88.16(7)	93.26(7)	
O(7) <sup>b</sup> -Mn(2)-O(8)	93.66(7)	93.37(7)	
O(8)-Mn(2)-O(8) <sup>b</sup>	180.00	180.00	
O(6) <sup>b</sup> -Mn(2)-O(7) <sup>b</sup>	75.48(7)	74.65(7)	
O(6) <sup>b</sup> -Mn(2)-O(8) <sup>b</sup>	91.84(7)	86.74(7)	
O(7) <sup>b</sup> -Mn(2)-O(8) <sup>b</sup>	86.34(7)	86.63(7)	
O(7)-Mn(2)-O(8)	86.34(7)	86.63(7)	
O(6) <sup>b</sup> -Mn(2)-O(7)	104.52(7)	105.35(7)	
Ni(2)-O(6)-Mn(2)	95.52(7)	95.83(8)	
Ni(2)-O(7)-Mn(2)	98.36(8)	95.87(7)	

<sup>b</sup> represents symmetry element 2-x,1-y,1-z in **1B**, -x,-4-y,-4-z in **2B**.

## Graphical Abstract

Three new trinuclear  $\text{Ni}^{\text{II}}\text{-Mn}^{\text{II}}$  complexes with various carboxylato bridges have been synthesized and characterized to explore the antiferromagnetic to ferromagnetic crossover angle for this system.

